Radiography 31 (2025) 102936

Contents lists available at ScienceDirect

Radiography

journal homepage: www.elsevier.com/locate/radi

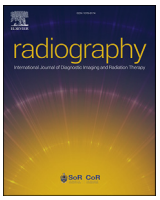

Exploring the impact of the female thoracic size, breast size and image receptor angles on the volume of missing breast tissue in mammographic imaging

R. Pape [a, *], X. Zheng [a], C. Cowling [b], C. West [c], A. Carstens [d, e], M. Kostidis [f], H. Bowmast [g]

[a] School of Dentistry and Medical Sciences, Discipline of Medical Radiation Science, Faculty of Science and Health, Charles Sturt University, Locked Bag 588, Building 30, Boorooma Street, Wagga Wagga, NSW, 2678, Australia
[b] Department of Medical Imaging and Radiation Sciences, School of Primary and Allied Health Care, Medicine, Nursing and Health Sciences, Monash University, Wellington Road, Clayton, Victoria, Australia
[c] Faculty of Science and Health, School of Nursing, Paramedicine and Healthcare Sciences, Charles Sturt University, Bathurst Campus, 353 Panorama Avenue, MITCHELL, NSW, 2795, Australia
[d] School of Animal, Environment and Veterinary Sciences, Veterinary School, Charles Sturt University, Locked Bag 588, Wagga Wagga, NSW, 2678, Australia
[e] Companion Animal Clinical Studies, Faculty of Veterinary Science, University of Pretoria, Onderstepoort, South Africa
[f] Austin Health, Repatriation Hospital Campus, 300 Waterdale Road, Heidelberg Heights, Victoria, Australia
[g] Department of Anatomy and Medical Imaging, Faculty of Medical and Health Sciences, The University of Auckland, Auckland, New Zealand

ARTICLE INFO

Article history:
Received 30 January 2025
Received in revised form
11 March 2025
Accepted 18 March 2025
Available online 8 April 2025

Keywords:
Female thorax
Breast volume
Breast cancer
Mammography positioning
Image receptor

ABSTRACT

Introduction: Optimal positioning in mammography and subsequent image quality can be impacted by thorax variability, breast size and the chosen image receptor (IR) angles. This study aims to explore the impact of the female thoracic size, breast size and IR angle on the volume of missing breast tissue (MBT) in mammographic imaging.
Methods: Sixty-three images were recorded: one craniocaudal (CC) at an IR angle of 0° for three sized breast phantoms attached to three sized thoracic models; and six mediolateral obliques (MLOs) at IR angles of 30°, 40°, 45°, 50°, 55°, 60° for three sized breast phantoms attached to three sized thorax models. Breast size was determined using the posterior nipple line (PNL) measurement and were recorded in millimetres. Breast volume was recorded in cubic centimetres.
Results: The breast size and breast tissue volume of a small thorax and large breasts was better visualised with increasing IR angles. Optimal MLO IR angles were determined for the combined average thorax with average breast at 55° and large thorax with large breast at 40° with minimum MBT values of 51.33 cm^3 and 75.07 cm^3, respectively. Female thoracic size, IR angle, and breast size are significant ($p < 0.01$) and have a positive impact on the volume of MBT.
Conclusion: Optimal MLO IR angles were determined for the three breast phantoms attached to three thoracic models. Female thoracic size positively impacts the volume of MBT and in terms of clinical practice it is vital to adjust the MLO IR angle to ensure maximum breast tissue coverage.
Implications for practice: These findings can be modelled in current clinical practice on women presented for mammography examinations with varying thorax and breast sizes, allowing optimal IR angle selection and therefore resulting in improved breast tissue inclusion and subsequently a more accurate breast cancer diagnosis.

Introduction

Breast cancer is a disease that affects millions of women worldwide and leads to death if not diagnosed and treated early. The World Health Organization (WHO) estimated that annually more than 500,000 women worldwide die from breast cancer.[1] Cancer develops when new abnormal cells, tissues or structures grow uncontrollably and deviate from the normal function of the breast. If not detected early, breast cancer may travel through the lymphatic and/or vascular systems and metastasise to other parts of the body, often resulting in death.[2] Mammography is central in breast cancer detection.

Mammographic imaging comprises two strategies: screening and diagnostic. Screening mammography was introduced in the

* Corresponding author.
E-mail address: rpape@csu.edu.au (R. Pape).

https://doi.org/10.1016/j.radi.2025.102936

1980's, targeting healthy women to check for early signs of breast cancer.[3] It is organised through systematic population-based screening programs and is undertaken at regular intervals to detect pre-clinical cancers.[1,2] Diagnostic mammography focuses on women with breast symptoms related to cancer and may trigger appropriate diagnostic investigations and treatment to improve outcomes.[1] Mammography is the most common imaging modality for the early detection of breast cancer and other breast diseases.[2] There are two routine positioning views in mammographic imaging. The craniocaudal (CC) view is the first routine view. It is perpendicular to the breast at an angle of 0° and clearly demonstrates most tissues of the breast,[4] excepting the most lateral regions of breast tissue.[5,6] The mediolateral oblique (MLO) view is the second routine view in mammography and when adequately performed, nearly all the breast tissue is imaged including the upper outer quadrant of the breast which is the location of the majority (over 75 %) of breast pathology.[7–10] Importantly, the MLO view uses a range of image receptor (IR) angles at 30°-70°[3–11] to maximise the inclusion of most breast tissue on the image. Although previous studies[12,13] reported a range of optimal IR angles at 40°-60° selected by radiographers during positioning for varied body habitus to maximise image quality, these same studies did not quantify the size and shape of female body habitus including the thorax to determine its impact on breast tissue inclusion. Whilst missing imaged tissue in the CC view can be improved by better positioning techniques and extended views,[3,7] it is only on the MLO view that the IR angle can make a difference in minimising the potential of missing breast tissue.[3–11] Optimal positioning in mammographic imaging is critical to the success of maximising breast tissue inclusion on the image and improve image quality.[3,7] However, optimal positioning in mammography and subsequent image quality evaluation (IQE) can be impacted by several anatomical factors including the female body habitus,[14–16] true thoracic size and its relationship to breast size[6,10,17] and the selection of optimum IR angles.[3–11]

Image quality evaluation (IQE) is undertaken using well-known criteria. These criteria have been formalised into image evaluation systems (IES) used by BreastScreen programs worldwide.[18–26] One such criteria is the posterior nipple line (PNL) measurement. Bassett et al.[7] defined the PNL measurement on the CC view as a reference line drawn directly posterior from the nipple to the pectoral muscle (PM) (Fig. 1A) or to the posterior edge of the image when the PM is not visualised (Fig. 1B). On the MLO view, Bassett et al.[7] defined the PNL as a reference line drawn at a 45° angle from the nipple extending to the anterior margin of the PM (Fig. 2A). The PNL measurement on the CC and the MLO images depict the two-dimensional size of the breast. This measurement is commonly used by the majority (70.8 %) of radiographers to evaluate image quality in the clinical setting.[27] The breast, due to differences in its anatomical presentation, cannot be imaged in its entirety at a single IR angle, which presents a unique challenge for IQE. Radiographers specialising in mammographic practice are taught to “standardise” their positioning so that the image is positioned the same the next time enabling an accurate comparison with previous images. Given the challenge of imaging the maximum volume of breast tissue for all women and the impact of the human body on the resultant image quality, there is the possibility of missing breast tissue in some patients even if all radiographers use the same or varied angle for MLOs. The aim of this study is to explore the impact of the female thoracic size, breast size and IR angle on the volume of missing breast tissue (MBT) in mammographic imaging.

Methods

Calculation of three female thoracic (rib cage) sizes

Calculation of three female thoracic (rib cage) sizes (small, average and large) were performed using a total of 347 computed tomography (CT) chest axial scans to determine statistical significance and were retrieved from the Medical Imaging and Data Resource Center (MIDRC) open access database[28] with exclusion criteria.[29] Calculations are detailed in Appendix A and B.

Calculation of three female breast sizes, weights and volumes

Calculation of three female breast sizes (small, average and large), weights and volumes using a total of 360 mammograms of a Chinese female screening population were downloaded from The Chinese Mammography Database (CMMD)[30] and are detailed in Appendix C.

Mammographic exposures of three thoracic models and three breast phantoms at selected IR angles

A Hologic Selena tomography machine (Hologic Incorporated, Bedford, MA, USA) with selection of 2D imaging was calibrated to give compression force in Newtons (N) with a 24 × 30 cm flexed and rigid paddle was used.[31] The breast phantom was compressed using the foot paddle then hand compression was applied to a pressure of approximately 50 N (48.2 N and 53.6 N).[31] The study recorded 63 exposures using 100–120 mAs and 28 kVp: one CC image at an angle of 0° for each small, average and large sized breast phantoms attached to small, average and large sized thoracic models; and six MLO images of each combination at angles of 30°, 40°, 45°, 50°, 55°, 60° for small, average and large sized breast phantoms attached to small, average and large sized thorax models. Since human breasts are usually almost visually symmetrical[10] and the phantom pair of breasts used for imaging were symmetrical, including the same amount of compression would be applied, exposures of both CC and MLO views were acquired with only one of the breast and CC in the right MLO position. The weight of one breast phantom of each size was then converted to volume of tissue using the standard formula that 1 g of breast tissue equals 1 cm^3 of tissue.[32,33] Hence, the total known volume of one breast phantom for each size acts as controls and include: a) small = 252 cm^3; b) medium = 402 cm^3; and c) large = 499 cm^3.

Results

PNL measurement and calculation of missing breast tissue by two mammography expert raters

Considering the absence of the pectoral muscle (PM) on the breast phantom images, two expert raters (Rater 1 [R1] & Rater 2 [R2]) in mammography with over 18 years of clinical experience, measured the PNL for both the CC view (Figs. 1B & 3A) and the MLO views (Figs. 2B & 3B) as defined by the American College of Radiology (ACR),[18] Bassett et al.[7] and the Royal Australian and New Zealand College of Radiologists (RANZCR)[25] independently and collaboratively. Both raters used their clinical experience to estimate a 45° angle to determine the PNL measurement on the MLO views (Figs. 2B & 3B). The inter-rater reliability of both raters is excellent with an intraclass correlation coefficient value of .976 [95 % CI .96–.985] for the single measures. The PNL measurements for both raters were quite similar with few mm's differences in

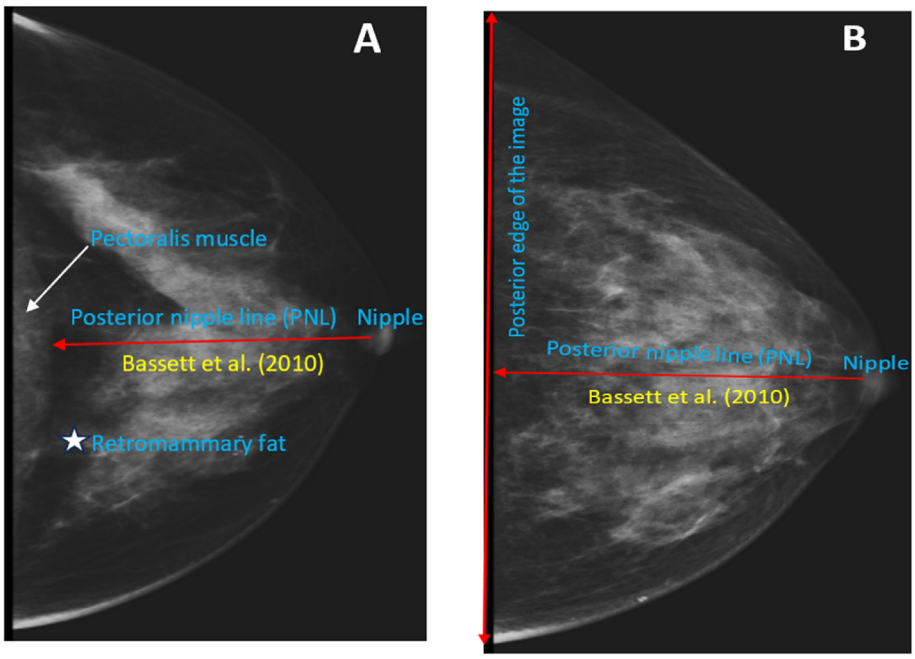

Figure 1. Posterior nipple line (PNL) measurement for the craniocaudal (CC) view. *(A)* Optimal positioning for the CC view demonstrates midline location of the nipple, inclusion of the pectoralis muscle (white arrow) on the image (some images may not include the pectoralis muscle), and depiction of retromammary fat (asterisk) posterior to the medial fibroglandular tissue. Note that some posterior lateral tissue often extends beyond the edge of the film. The PNL is drawn directly posterior from the nipple to the muscle; *(B)* or to the posterior edge of the image when the muscle is not visualized.[7] Source: Images A & B adapted from The Chinese Mammography Database (CMMD).[30]

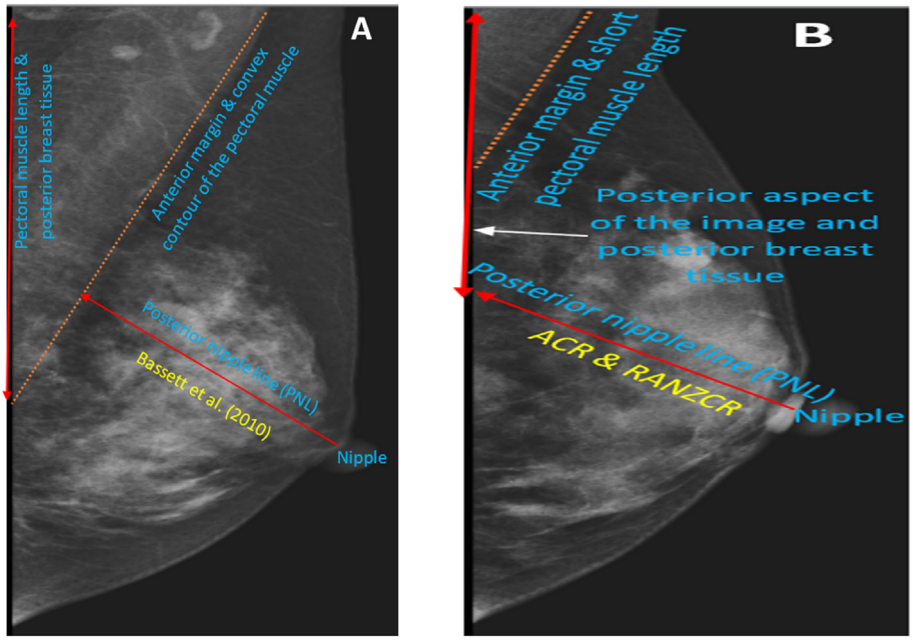

Figure 2. Posterior nipple line (PNL) measurement for the mediolateral oblique (MLO) view. *(A)* The PNL is drawn at a 45° angle from the nipple extending to the anterior margin of the pectoralis muscle[7]; *(B)* or to the posterior aspect of the image whichever comes first.[18,25] Source: Images A, B & C adapted from The Chinese Mammography Database (CMMD).[30] Note: ACR, American College of Radiology[18]; RANZCR, The Royal Australian and New Zealand College of Radiologists.[25]

missing breast tissue (MBT) (Table 3). The majority (n = 60) of the volume values of differences in MBT rated by R1 and R2 were below the total known volume values of breast tissue for the small (252 cm^3), average (402 cm^3) and large (499 cm^3) size breast phantoms and were considered optimal values (Table 3). Hence an average value of both rater's PNL measurements were calculated using the formula: PNL value for Rater 1 + PNL value for Rater 2 divided by 2 (Table 1).

Breast phantom volume calculation

The current study calculated breast volume using both the CC and MLO views and were recorded in cubic millimetre (mm^3). To convert mm^3 to cubic centimetre (cm^3), the standard formula was used: 1 mm^3 = .001 cm^3 or the volume values were divided by 1000. Considering the breast shape as being oval, volume for the CC view was based on the algebraic formula of a circular

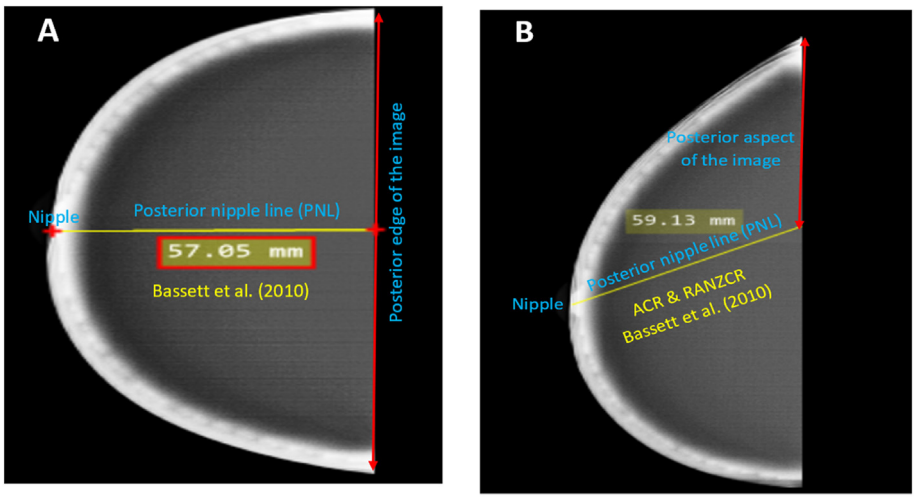

Figure 3. Posterior nipple line (PNL) measurement for the craniocaudal (CC) view *(A)* and the mediolateral oblique (MLO) view *(B)* on the breast phantom images. *(A)* The PNL is drawn directly posterior from the nipple to the posterior edge of the image when the pectoral muscle is not visualized.[7] *(B)* The PNL is drawn at a 45° angle from the nipple extending to the posterior aspect of the image as the anterior margin of the pectoral muscle is not visualized.[7,18,25] Note: ACR, American College of Radiology[18]; RANZCR, The Royal Australian and New Zealand College of Radiologists.[25]

Table 1
Shows the PNL measurements of three breast phantoms and three thorax model sizes relative to CC and MLO IR angles by two raters in x-ray mammographic imaging.

CC view (1×) vs MLO views (6×)	LTLB	LTMB	LTSB	MTLB	MTMB	MTSB	STLB	STMB	STSB
CC vs MLO IR angle	PNL (mm)	PNL (mm)	PNL (mm)	PNL (mm)	PNL (mm)	PNL (mm)	PNL (mm)	PNL (mm)	PNL (mm)
CC 0° (R1+R2/2) *	44.04	46.06	32.29	53.87	42.98	32.08	57.39	44.11	28.12
MLO 30° (R1+R2/2) *	57.95	55.23	38.67	61.78	57.47	44.1	70.33	62.66	53.84
MLO 40° (R1+R2/2) *	67.74	62.76	43.69	64.95	60.21	49.08	72.36	64.56	53.12
MLO 45° (R1+R2/2) *	55.76	62.17	44.64	65.18	60.47	46.99	71.05	64.69	53.5
MLO 50° (R1+R2/2) *	61.83	63.51	42.83	64.75	61.82	49.59	69.65	68.48	55.13
MLO 55° (R1+R2/2) *	59.92	64.39	54.41	67.11	63	51.55	71.28	67.71	54.48
MLO 60° (R1+R2/2) *	59.60	66.93	52.44	67.60	62.44	53.23	72.78	66.37	53.73

Abbreviation: CC, craniocaudal; MLO, mediolateral oblique; IR, image receptor; PNL, posterior nipple line; mm, millimetre; LTLB, large thorax large breast; LTMB, large thorax medium breast; LTSB, large thorax small breast; MTLB, medium thorax large breast; MTMB, medium thorax medium breast; MTSB, medium thorax small breast; STLB, small thorax large breast; STMB, small thorax medium breast; STSB, small thorax small breast; R1+R2/2*, Average calculation (Rater 1 plus Rater 2 divided by 2).

base using the Katariya et al.[34] method: volume = Pi (3.14) x (radius CC)^2 x height (PNL CC)/3 (Table 2). The PNL represented the breast height, the breast width (BW) represented the distance from the most lateral point of breast tissue to the most medial point of breast tissue, and the radius was recorded as half the BW[32,34] (Fig. 4). Volume for the MLO view used the same calculations as the CC view except BW was defined as the distance from the most inferior aspect of the breast tissue to the junction between the most superior aspect of the breast tissue at the posterior edge of the image (Fig. 5). Shanley et al.[32] defined their BW as the distance from the most inferior point of breast tissue to the most superior point of breast tissue including that beyond the thoracodorsal artery. The differing methods in BW calculation in the current study compared to the Shanley et al.[32] is due to the absence of a PM on the breast phantom.

Table 2
Shows the volumes of three breast phantoms and three thorax model sizes relative to CC and MLO IR angles by two raters in x-ray mammographic imaging.

CC view (1×) vs MLO views (6×)	LTLB	LTMB	LTSB	MTLB	MTMB	MTSB	STLB	STMB	STSB
CC vs MLO IR angle	Volume (cm^3)	Volume (cm^3)	Volume (cm^3)	Volume (cm^3)	Volume (cm^3)	Volume (cm^3)	Volume (cm^3)	Volume (cm^3)	Volume (cm^3)
CC 0° (R1+R2/2) *	186.92	203	102.94	236.32	180.68	105.09	235.51	190.79	88.18
MLO 30° (R1+R2/2) *	325.27	289.81	151.10	374.43	322.57	198.94	417.94	319.03	245.43
MLO 40° (R1+R2/2) *	423.93	342.14	191.66	416.09	337.95	225.50	444.04	334.43	249.70
MLO 45° (R1+R2/2) *	332.72	333.22	201.37	399.93	342.24	227.92	437.66	342.38	249.20
MLO 50° (R1+R2/2) *	396.10	337.55	189.66	413.17	339.82	232.03	434.14	348.66	259.14
MLO 55° (R1+R2/2) *	364.73	339.31	268.63	415.06	350.67	241.20	440.85	341.68	239.00
MLO 60° (R1+R2/2) *	361.36	345.23	265.81	419.72	338.98	238.99	423.82	332.03	229.13

Abbreviation: CC, craniocaudal; MLO, mediolateral oblique; IR, image receptor; Volume in cm^3, cubic centimetre; LTLB, large thorax large breast; LTMB, large thorax medium breast; LTSB, large thorax small breast; MTLB, medium thorax large breast; MTMB, medium thorax medium breast; MTSB, medium thorax small breast; STLB, small thorax large breast; STMB, small thorax medium breast; STSB, small thorax small breast; R1+R2/2*, Average calculation (Rater 1 plus Rater 2 divided by 2).
Note: a. Formula for volume of a circular base (breast shape): Volume = Pi (3.14) x (radius CC/MLO)^2 x height (PNL CC/MLO)/3[32,34].
b. To convert mm^3 to cm^3, the standard formula was used: 1 mm^3 = .001 cm^3 or the volume values were divided by 1000.

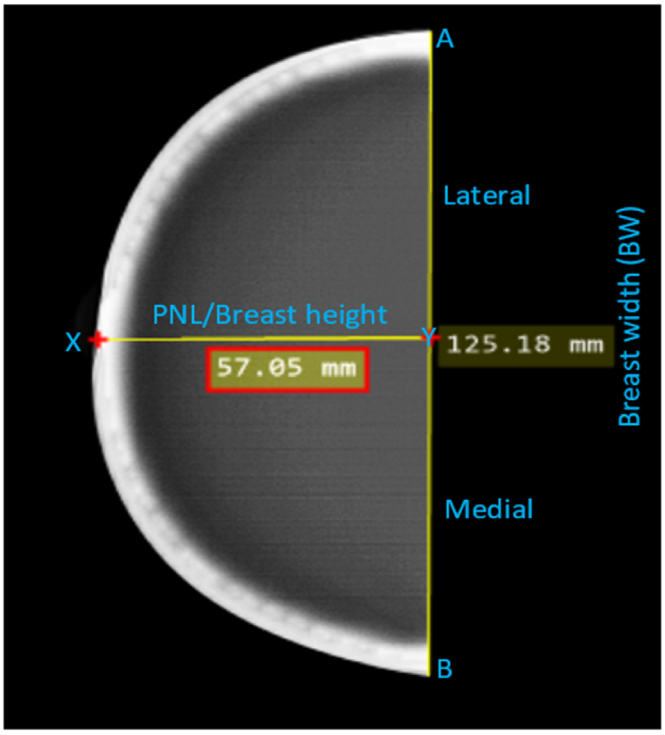

Figure 4. Breast phantom demonstrating measurements needed to calculate volume of breast tissue on the craniocaudal (CC) view including the posterior nipple line (PNL) or breast height (distance = X to Y) and the BW (distance = A to B).

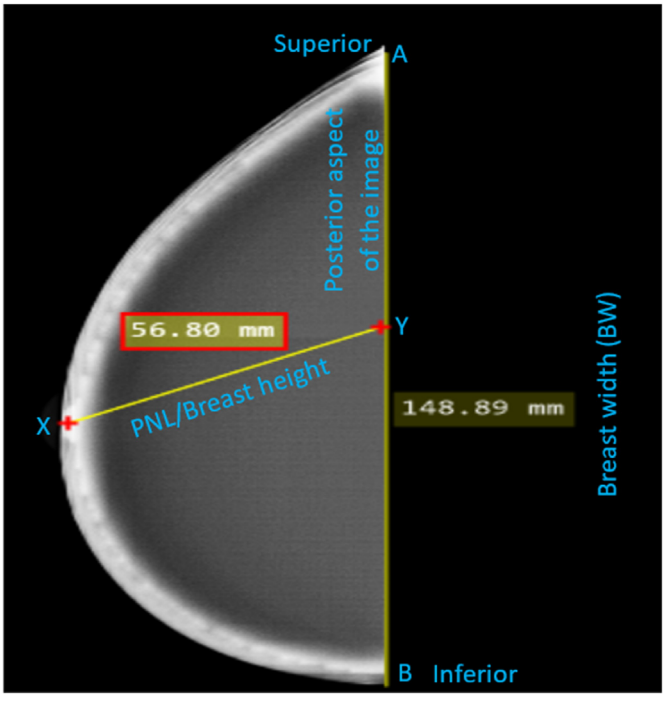

Figure 5. Breast phantom demonstrating measurements needed to calculate volume of breast tissue on the mediolateral oblique (MLO) view including the posterior nipple line (PNL) or breast height (distance = X to Y) and the BW (distance = A to B).

The impact of IR angles, thorax sizes and breast sizes on the volume of missing breast tissue

The linear regression analysis (Table 4) tests were undertaken to show the impact of image receptor (IR) angles, thorax sizes and breast sizes on the volume of missing breast tissue (MBT). IR angle impact is significant ($p < 0.01$), and the study hypothesis is accepted. IR angle has a positive impact on the volume of MBT. Thorax size has a positive impact on the volume of MBT, demonstrating a significant impact ($p < 0.01$), as was hypothesised by this study. The impact of breast size is also significant ($p < 0.01$), demonstrating that breast size has a positive impact on the volume of MBT.

Discussion

Body habitus, breast size and breast tissue volume

This study determined the breast size and breast tissue volume (BTV) of three breast phantoms attached to three thoracic model sizes after imaging individually using the CC and MLO IR angles. The findings revealed that for all seven IR angles (one CC and six MLO), the breast size and BTV demonstrated for a small thorax and large breast combination was increased with increasing IR angles (Tables 1 and 2). Although most women may have a slight variation in breast symmetry, indicating that the size, volume, shape and position on the thoracic wall varies slightly from right to left,[10] the findings in this study showed that the breast size and BTV demonstrated for a small thorax and large breast was increased with increasing IR angles. Recent studies revealed that body habitus affects radiographic image quality,[35,36] and specifically women exhibiting a larger body habitus may produce poor mammographic image quality.[15] However, these same studies do not confirm that women with larger body habitus have larger breast size or women with smaller body habitus have smaller breast size. Generally, it is expected that women exhibiting a smaller body habitus may have smaller breast sizes and subsequently produce good quality images. However, another study contradicts this perception indicating that women with larger body habitus may have small breasts that spread laterally around the wider curved thorax, and additional mammographic views such as an exaggerated CC or a CC with slight oblique may be required to adequately image missing lateral tissue.[15] Importantly, the findings in this study align with the mammography literature documenting a range of MLO IR angles[3–11] preferred to image a small thorax and large breast at 55° and 60° IR angles which demonstrated increased breast size and BTV whilst a large thorax and small breast demonstrated decreased breast size and BTV at 30°, 40° and 45° IR angles. These findings suggest that the preferred range of MLO IR angles for a small thorax (55° and 60°) and a large thorax (30°, 40° and 45°) used in this study could minimise the potential of missing breast tissue in women with an increased or decreased breast size and BTV, respectively, and subsequently enhance early breast cancer detection.

Volume of missing breast tissue and optimal IR angle

In this study, volume of missing breast tissue (MBT) for the three female breast phantoms attached to the three thorax models were determined by calculating the difference of the average volume of the small, average and large breast images for rater 1 (R1) and rater 2 (R2) from the total known volume of the small, average (medium) and large breast phantoms (Table 3). Although the pectoral muscle (PM) was not captured on both the CC and MLO breast phantom images, this (absence of PM) did not fail to demonstrate the potential of MBT and its impact on thoracic curvature. The findings highlighted in Table 3 revealed optimal MLO IR angles for the three breast phantoms attached to the three thorax models with minimum MBT. Particularly, optimal MLO IR angles were determined for the combined small thorax with small breast (40°), average thorax with average breast (55°) and large thorax with large breast (40°) with minimum MBT. These findings are novel in mammographic

Table 3
Shows the volume of missing breast tissue of three breast phantoms and three thorax model sizes relative to CC and MLO IR angles by two raters in x-ray mammographic imaging.

CC view (1×) vs MLO views (6×)	LTLB	LTMB	LTSB	MTLB	MTMB	MTSB	STLB	STMB	STSB
CC vs MLO IR angle	Volume MBT (cm^3)	Volume MBT (cm^3)	Volume MBT (cm^3)	Volume MBT (cm^3)	Volume MBT (cm^3)	Volume MBT (cm^3)	Volume MBT (cm^3)	Volume MBT (cm^3)	Volume MBT (cm^3)
CC 0° (R1+R2/2) *	312.08	199	149.06	262.68	221.32	146.91	263.49	211.21	163.82
MLO 30° (R1+R2/2) *	173.73	112.19	100.9	124.57	79.43	53.06	81.06	82.97	6.57
MLO 40° (R1+R2/2) *	75.07	59.86	60.34	82.91	64.05	26.5	54.96	67.57	2.3
MLO 45° (R1+R2/2) *	166.28	68.78	50.63	99.07	59.76	24.08	61.34	59.62	2.8
MLO 50° (R1+R2/2) *	102.9	64.45	62.34	85.83	62.18	19.97	64.86	53.34	−7.14
MLO 55° (R1+R2/2) *	134.27	62.69	−16.63	83.94	51.33	10.8	58.15	60.32	13.0
MLO 60° (R1+R2/2) *	137.64	56.77	−13.81	79.28	63.02	13.01	75.18	69.97	22.87

Abbreviation: a. CC, craniocaudal; MLO, mediolateral oblique; IR, image receptor; Volume in cm^3, cubic centimetre; LTLB, large thorax large breast; LTMB, large thorax medium breast; LTSB, large thorax small breast; MTLB, medium thorax large breast; MTMB, medium thorax medium breast; MTSB, medium thorax small breast; STLB, small thorax large breast; STMB, small thorax medium breast; STSB, small thorax small breast; MBT, missing breast tissue; R1+R2/2*, Average calculation (Rater 1 plus Rater 2 divided by 2).
Note: a. The total known volume of one breast phantom for each size include: a) Large = 499 cm^3; b) medium = 402 cm^3; and c) small = 252 cm^3.
b. To determine the MBT by the three thorax sizes (large, medium and small) for each IR angles, calculate the difference of the average volume of the large, medium and small breast images for R1 and R2 from the total known volume of the large, medium and small breast phantoms.
c. Light gold colour demonstrates optimal MLO IR angles for the three breast phantoms attached to the three thorax models with minimum MBT.

imaging and may reflect the amount of breast tissue not demonstrated in real female breasts attached to a real female thorax. The CC IR angle at 0° is always defined as perpendicular to the breast and whilst MBT in the CC view can be improved by better positioning skills and an extended CC view,[3–11,15] it is only on the MLO view that the IR angle can make a difference to maximise the potential of breast tissue inclusion on the image. Although the mammography literature documents that a variety of MLO IR angles at 30°-70°[3-11] are selected for individuals with varied body habitus and varied breast sizes, the findings of this study have demonstrated a quantified definition of optimal MLO IR angle for specific female thoracic sizes, breast sizes and MBT. Hence, further research using these documented optimal MLO IR angles for each individual body habitus and specific breast sizes as experienced routinely in the clinical setting representing the wider mammography screening population should be undertaken to validate these findings.

The impact of volume of missing breast tissue (MBT) on IR angles, thorax sizes and breast sizes

In this study, the linear regression analysis (Table 4) was undertaken to show the impact of image receptor (IR) angles, thorax sizes and breast sizes on the volume of missing breast tissue (MBT). The IR angle selected has a significant impact ($p < 0.01$), indicating that IR angle has a positive impact on the volume of MBT imaged. This result demonstrated that as the IR angle increases, the volume of breast tissue not demonstrated on the image also increases. Thorax size also has a significant positive impact on the volume of MBT ($p < 0.01$). This result demonstrated that female body habitus (thorax size) affects the volume of breast tissue not demonstrated and that in terms of clinical practice it is vital to adjust the IR angle on the MLO to ensure maximum breast tissue coverage. Breast size impact on MBT was also found to be significant ($p < 0.01$), indicating that breast size has a positive impact on the volume of MBT. This result demonstrated that as the breast size increases, the volume of breast tissue not demonstrated on the image also increases. These findings are novel in mammographic imaging and confirm that female body habitus,[14–16] true thoracic size and its relationship to breast size[6,10,17] and the selection of optimal IR angles[3–11] impact the amount of breast tissue not demonstrated on the image. These findings should be applicable to current clinical practice on real women presenting for mammographic examination to enhance the potential of maximising breast tissue inclusion.

Strengths and limitations

This is the first study adding to the limited body of mammography knowledge by demonstrating that the IR angle, female model thoracic size, and breast size are significant and have a positive impact on the volume of MBT in mammographic imaging. Furthermore, this study documented the optimal MLO IR angle with minimum MBT for each of the three breast phantoms attached to the three thoracic models. The limitations in the study acknowledge that the 63 images captured include female breast phantoms attached to female thoracic models and may not reflect real female breasts or the real female thorax which can limit the accuracy and generalisability of the findings. This was mitigated through a rigorous experimental study design, data collection, reliability of breast size measurement using expert raters, and data analysis process. The role of the expert raters as mammographers may be a potential bias in this study. Finally, the databases used for thorax shapes and breast sizes reflect White Caucasian, Black or African American and Chinese female population which may not represent a wider global female population.

Table 4
The linear regression analysis table to show the impact of image receptor (IR) angles, thorax sizes and breast sizes on the volume of missing breast tissue (MBT).

Coefficients[a]						
Model		Unstandardized Coefficients		Standardized Coefficients	t	Sig.
		B	Std. Error	Beta		
1	(Constant)	82.628	15.182		5.443	<0.001
	Angles	−2.682	0.194	−0.751	−13.854	<0.001
	Thorax	16.592	4.436	0.203	3.740	<0.001
	Breast	38.398	4.436	0.470	8.657	<0.001

[a] Dependent Variable: Volume (MBT).

Implications for practice

This study facilitated a good understanding of the female body habitus, thoracic size, breast size, IR angles and how these impact on the volume of MBT on the resultant mammographic image. In terms of clinical relevance, a chart of the optimal MLO IR angles for each of the three breast phantom sizes attached to the three thoracic model sizes can be created and displayed within the mammography room, acting as a quick guide for practitioners to determine which IR angle is best served for the current patient. This would improve breast tissue inclusion and reduce MBT, improving image quality and subsequently breast cancer detection.

Conclusion

This experimental study proved the hypothesis that IR angle, female thoracic size and breast size have a positive impact on the volume of breast tissue not demonstrated on the image. The study documented optimal MLO IR angles for the combined small thorax with small breast (40°), average thorax with average breast (55°) and large thorax with large breast (40°) with minimum MBT. Importantly, the results in this study demonstrated that female body habitus (thorax size) positively impacts the volume of breast tissue not demonstrated on the image. Future recommendations for clinical practice is to emphasise the importance of adjusting the MLO IR angle to ensure maximum breast tissue coverage and subsequent breast cancer diagnosis. Finally, future studies should be undertaken to validate findings of this study on real-world clinical imaging data.

Informed consent statement

The CT chest images, and breast mammography images used in this work are in public domain, and access to these databases was approved by the database owners. As such, informed consent was obtained before data collection by the respective database owners.

Data availability statement

The original CT chest image data were downloaded from the Medical Imaging and Data Resource Center (MIDRC) database (https://www.midrc.org) (accessed on 13 January 2024). The original breast mammography image data were downloaded from The Chinese Mammography Database (CMMD) (https://doi.org/10.7937/tcia.eqde-4b16) (accessed on 13 January 2024). The processed data is available upon request from the author.

Ethics statement

The CT chest images, and breast mammography images used in this work are in public domain, and access to these databases was approved by the database owners. As such: (1) the institutional ethics approval was exempted by Charles Sturt University's Human Research Ethics Committee; (2) the methods used in this study are in accordance with the guidelines of Charles Sturt University's Human Research Ethics Committee.

The experimental study of phantoms was approved by the Charles Sturt University Radiation Safety Committee (02/09/24, approval number: R24006RP).

Author contributions

Ruth Pape: Conceptualisation, Methodology, Formal analysis, Investigation, Writing - original draft, Writing - review & editing. **Xiaoming Zheng**: Formal analysis, Writing – review & editing. **Cynthia Cowling**: Writing - review & editing. **Caryn West**: Writing - review & editing. **Ann Carstens**: Writing - review & editing. **Michelle Kostidis**: Methodology, Formal analysis, Writing - review & editing. **Heidi Bowmast**: Methodology, Writing - review & editing. All authors have read and agreed to the published version of the manuscript.

Acknowledgement

CT chest data used in preparation of this article were obtained from the Medical Imaging and Data Resource Center (MIDRC) database (https://www.midrc.org). As such, the investigators within the MIDRC contributed to the design and implementation of MIDRC and/or provided data but did not participate in analysis or writing of this report. A complete listing of MIDRC investigators can be found at: https://www.midrc.org/midrc-team.

Breast mammography data used in preparation of this article were obtained from The Chinese Mammography Database (CMMD) (https://doi.org/10.7937/tcia.eqde-4b16). As such, the investigators within the CMMD contributed to the design and implementation of CMMD and/or provided data but did not participate in analysis or writing of this report. A complete listing of CMMD investigators can be found at: https://doi.org/10.7937/tcia.eqde-4b16.

All authors sincerely acknowledge the Mammography department at the Heidelberg Repatriation Hospital and Austin Health in Melbourne, Australia for their support in using their mammography equipment in performing this experimental study. We sincerely acknowledge Michelle Kostidis, an experienced radiographer and clinical expert in mammography for supervision in this experimental study. This research was funded through the Australian Awards Scholarship as part of the first author's (RP) PhD Program at Charles Sturt University. The author very much appreciates and acknowledges the Australian Award Scholarship for funding this doctoral research study.

Appendix A. Supplementary data

Supplementary data to this article can be found online at https://doi.org/10.1016/j.radi.2025.102936.

References

1. World Health Organisation. *WHO position paper on mammography screening*. WHO Press; 2014. Available at: https://www.who.int/publications/i/item/who-position-paper-on-mammography-screening. [Accessed 18 January 2025].
2. Tabár L, Tot T, Dean PB. A new era in the diagnosis and treatment of breast cancer. In: Tabár L, Tot T, Dean PB, editors. *Breast cancer: the art and science of early detection with mammography. Perception, interpretation, histopathologic correlation*, **1**. Stuttgart: Georg Thieme Verlag; 2005. p. 166–235.
3. Long SM, Miller LC, Botsco MA, Martin LL. *The handbook of mammography*. 5th ed. Mammography Consulting Services Ltd; 2010.
4. Peart O. Positioning challenges in mammography. *Radiol Technol* 2014;**85**(4): 417M–43M.
5. Lee L. Mammography: basic projections. In: Lee L, Stickland V, Wilson R, Evans A, editors. *Fundamentals of mammography*. 2nd ed. Elsevier Science Limited; 2003. p. 31–46.
6. Peart O. *Mammography and breast imaging: just the facts*. The McGraw-Hill Companies, Inc; 2005.
7. Bassett LW, Hoyt AC, Oshiro T. Digital mammography: clinical image evaluation. *Radiol Clin* 2010;**48**(5):903–15. https://doi.org/10.1016/j.rcl.2010.06.006.
8. Eklund GW. The art of mammographic positioning. In: al MFe, editor. *Radiological diagnosis of breast diseases*. Springer-Verlag Berlin Heidelberg; 2000. p. 75–88.
9. Eklund GW, Cardenosa G, Parsons W. Assessing adequacy of mammographic image quality. *Radiology* 1994;**190**(2):297–307. https://doi.org/10.1148/radiology.190.2.8284372.
10. Darlington AJ. Anatomy of the breast. In: Hogg P, Kelly J, Mercer C, editors. *Digital mammography: a holistic approach*. Springer International Publishing; 2015. p. 3–10. https://doi.org/10.1007/978-3-319-04831-4_1.
11. Mercer CE, Hill CA, Kelly A, Smith HL. Practical mammography. In: Hogg P, Kelly J, Mercer C, editors. *Digital mammography: a holistic approach*. Springer International Publishing; 2015. p. 175–88. https://doi.org/10.1007/978-3-319-04831-4_1.

12. Pape R. Australian radiographers' digital era practice in selecting the image receptor angle for female body habitus for the mediolateral oblique view of the breast. *Radiography* 2024;**30**(6):1612–21. https://doi.org/10.1016/j.radi.2024.10.001.
13. Spuur K, Poulos A. Mammography: current practice in Australia for the selection of bucky angle in the mediolateral oblique view of the breast. *Eur J Radiogr* 2009;**1**(4):115e23. https://doi.org/10.1016/j.ejradi.2010.02.001.
14. Rajapakse CS, Chang G. Impact of body habitus on radiologic interpretations. *Acad Radiol* 2014;**21**(1):1–2. https://doi.org/10.1016/j.acra.2013.10.006.
15. Destounis S, Newell M, Pinsky R. Breast imaging and intervention in the overweight and obese patient. *Am J Roentgenol* 2011;**196**(2):296–302. https://doi.org/10.2214/AJR.10.5556.
16. Elmore JG, Carney PA, Abraham LA, Barlow WE, Egger JR, Fosse JS, et al. The association between obesity and screening mammography accuracy. *Arch Intern Med* 2004;**164**(10):1140–7. https://doi.org/10.1001/archinte.164.10.1140.
17. Pemberton J, Ng YY. The normal breast. In: Tucker AK, Ng YY, editors. *Textbook of mammography*. 2nd ed. Churchill Livingstone-Harcourt Publishers Limited; 2001. p. 79–93.
18. American College of Radiology. *Mammography quality control manual*. American College of Radiology; 1999. Available at: https://www.acr.org/-/media/ACRAccreditation/Documents/Mammography/1999_Mammo_QCManual_Book_final.pdf.
19. BreastScreen Australia. *BreastScreen Australia National Accreditation standards*. Commonwealth of Australia Printing Press; 2019. Available at: https://www.health.gov.au/sites/default/files/documents/2019/09/breastscreen-australia-national-accreditation-standards-nas-breastscreen-australia-national-accreditation-standards.pdf.
20. Borrelli C, Dale M, Jenkins J, Kelly J, Vegnuti Z, Whelehan P. *Breast screening program guidance for breast screening mammographers*. Public Health England; 2017. Available at: https://iperforms.com/performs/wp-content/uploads/sites/3/2020/04/NHS_Breast_Screening_Programme_Guidance_for_mammographers.pdf.
21. Hofvind S, Vee B, Sørum R, Hauge M, Ertzaas A-KO. Quality assurance of mammograms in the Norwegian breast cancer screening program. *Eur J Radiogr* 2009;**1**(1):22–9. https://doi.org/10.1016/j.ejradi.2008.11.002.
22. Ministry of Health. *BreastScreen Aotearoa National Policy and quality standards*. Ministry of Health; 2013. Available at: https://www.nsu.govt.nz/system/files/page/breastscreen_aotearoa_national_policy_and_quality_stardards.pdf.
23. National Health Service Breast Cancer Screening Program. *National quality assurance coordinating group for radiography: quality assurance guidelines for mammography including radiographic quality control*. NHS Cancer Screening Programmes; 2006 (Publication No. 63).
24. Perry N, Broeders M, de Wolf C, Tornberg S, Holland R, von Karsa L. *European guidelines for quality assurance in breast cancer screening and diagnosis*. European Communities; 2006. https://screening.iarc.fr/doc/ND7306954ENC_002.pdf.
25. Royal Australian and New Zealand College of Radiologists. *Mammography Quality Control Manual Royal Australian and New Zealand College of Radiologists*. 2002.
26. Wadden NAT, Hapgood C. Canadian association of Radiologists mammography Accreditation Program—clinical image assessment. *Can Assoc Radiol J* 2022;**73**(1):157–63. https://doi.org/10.1177/08465371211025195.
27. Bentley K, Poulos A, Rickard M. Mammography image quality: analysis of evaluation criteria using pectoral muscle presentation. *Radiography* 2008;**14**(3):189–94. https://doi.org/10.1016/j.radi.2007.02.002.
28. MIDRC. *Medical imaging and data resource center*. 2025. Available at: https://www.midrc.org. [Accessed 13 January 2025].
29. Spuur K, Hung WT, Poulos A, Rickard M. Mammography image quality: model for predicting compliance with posterior nipple line criterion. *Eur J Radiol* 2011;**80**(3):713–8. https://doi.org/10.1016/j.ejrad.2010.06.026.
30. Cui Chunyan, Li Li, Cai Hongmin, Fan Zhihao, Zhang Ling, Dan Tingting, et al. The Chinese Mammography Database (CMMD): an online mammography database with biopsy confirmed types for machine diagnosis of breast. *Cancer Imaging Arch* 2021. https://doi.org/10.7937/tcia.eqde-4b16.
31. Ma WK, Hogg P, Kelly J, Millington S. A method to investigate image blurring due to mammography machine compression paddle movement. *Radiography* 2015;**21**(1):36–41. https://doi.org/10.1016/j.radi.2014.06.004.
32. Shanley E, Johnston A, Hillick D, Ng KC, Sugrue M. Digital breast volume estimation (DBVE)—a new technique. *Br J Radiol* 2018;**91**(1091):20180406. https://doi.org/10.1259/bjr.20180406.
33. Parmar C, West M, Pathak S, Nelson J, Martin L. Weight versus volume in breast surgery: an observational study. *JRSM Short Rep* 2011;**2**:1–5. https://doi.org/10.1258/shorts.2011.011070.
34. Katariya RN, Forrest AP, Gravelle IH. Breast volumes in cancer of the breast. *Br J Cancer* 1974;**29**:270–3. https://doi.org/10.1038/bjc.1974.66.
35. Hardy M, Scotland B, Herron L. Assessing sagittal rotation on posteroanterior chest radiographs: the effect of body morphology on radiographic appearances. *J Med Imag Radiat Sci* 2015;**46**(4):365–71. https://doi.org/10.1016/j.jmir.2015.07.004.
36. Ogoke A, Ugwu A, Ugwuanyi D, Ohagwu C, Ogolodom M. The impact of body habitus and body mass index on rotation in chest radiographs: a single center study. *Arch Med* 2020;**12**(1):2. https://www.researchgate.net/profile/Christopher-Ohagwu-2/publication/340735352.